Bidirectional quantum teleportation of unknown photons using path-polarization intra-particle hybrid entanglement and controlled-unitary gates via cross-Kerr nonlinearity*

Jino Heo[a)b)], Chang-Ho Hong[a)b)], Jong-In Lim[a)b)], and Hyung-Jin Yang[a)c)†]

[a)] *Graduate School of Information Security (GSIS), Korea University, Anam 5-ga Sungbuk-gu, Seoul, Republic of Korea*
[b)] *Center for Information Security Technologies (CIST), Korea University, Seoul, Republic of Korea*
[c)] *Department of Physics, Korea University, Sejong* 339-700, *Republic of Korea*

(Received 14 July 2014; revised manuscript received 21 October 2014; published online 27 March 2015)

We propose an arbitrary controlled-unitary (CU) gate and a bidirectional quantum teleportation (BQTP) scheme. The proposed CU gate utilizes photonic qubits (photons) with cross-Kerr nonlinearities (XKNLs), X-homodyne detectors, and linear optical elements, and consists of the consecutive operation of a controlled-path (C-path) gate and a gathering-path (G-path) gate. It is almost deterministic and feasible with current technology when a strong coherent state and weak XKNLs are employed. Based on the CU gate, we present a BQTP scheme that simultaneously teleports two unknown photons between distant users by transmitting only one photon in a path-polarization intra-particle hybrid entangled state. Consequently, it is possible to experimentally implement BQTP with a certain success probability using the proposed CU gate.

Keywords: cross-Kerr nonlinearity, bidirectional quantum teleportation, intra-particle hybrid entanglement

PACS: 03.67.−a, 42.50.Ex, 42.65.−k, 03.67.Hk **DOI:** 10.1088/1674-1056/24/5/050304

1. Introduction

Quantum teleportation (QTP) is a quantum information processing protocol[1–46] through which an unknown quantum state is teleported from a sender to a receiver using an entangled state, which is employed as a quantum channel between distant users. In QTP, the sender does not directly transmit the unknown photon; therefore, the receiver has to reconstruct its state using appropriate unitary operators. Since the first unidirectional quantum teleportation (UQTP) was introduced by Bennett *et al.*,[2] many modified QTP schemes have been proposed[10–22,34–39] and implemented experimentally.[15–17,34–39]

Recently, bidirectional quantum controlled teleportation (BQCTP) schemes using a five-qubit Brown state,[23] five-qubit cluster state,[24] five-qubit composite GHZ-Bell state,[25] five-qubit state,[26] and six-qubit cluster state[27] have been proposed. These are simultaneous teleportation schemes that are used for teleporting two unknown quantum states between users who regain the initial states. In these schemes, a user simultaneously becomes both the message sender and the message receiver.

Some of the aforementioned schemes[1–39] employ inter-particle entangled states, which are entangled states with the same degrees of freedom in two or more particles, such as spin. In contrast, hybrid entanglement is a correlation between different degrees of freedom, such as path, polarization, linear momentum, and spin.[47,48] An even more interesting phenomenon is the intra-particle hybrid entanglement, which is the hybrid entanglement within a single particle. The possibilities of the involvement of various types of degrees of freedom, such as the polarization and linear momentum,[49,50] the polarization and angular momentum[51] of a single photon, and the path and spin[52] of a single neutron, have been theoretically and experimentally investigated. Intra-particle hybrid entanglement has an advantage of efficiency over inter-particle entanglement because intra-particle hybrid entanglement is a correlation within a single particle. Thus, it can be more easily preserved against dissipative effects. Consequently, the quantum information processing protocols using intra-particle hybrid entanglement are less influenced by noise and consume fewer resources than those using inter-particle entanglement. Recently, various quantum information processing protocols using intra-particle hybrid entanglement, such as entanglement swapping,[43] quantum key distribution (QKD),[44] UQTP,[45] and unidirectional quantum direct transmission,[46] have been demonstrated. However, bidirectional quantum teleportation (BQTP) protocols using intra-particle hybrid entanglement have not so far been demonstrated by transmitting only one photon.

For the experimental realization of BQTP (and QTP) with a certain success probability, quantum controlled-unitary (CU) gates play a very important role. Accordingly, the deterministic CU gates must be realized with experimental feasibility. The cross-Kerr nonlinearity (XKNL) effects have been

*Project supported by the Ministry of Science, ICT&Future Planning, Korea, under the C-ITRC (Convergence Information Technology Research Center) Support program (NIPA-2013-H0301-13-3007) supervised by the National IT Industry Promotion Agency.

†Corresponding author. E-mail: yangh@korea.ac.kr

© 2015 Chinese Physical Society and IOP Publishing Ltd

well studied, both experimentally and theoretically. In principle, the XKNL effect can induce efficient photon interactions with which photonic gates can be implemented, using far fewer physical resources than linear optical schemes. For the giant nonlinearity, the strong XKNL can be used directly to implement multi-qubit gates.[53,54] Although considerable progress has been made, the experimental implementation of strong XKNL is still difficult.[55] For this reason, later works endeavored to obtain multi-qubit gates by utilizing the weak XKNL.[56–64] Nemoto *et al.* proposed nearly deterministic controlled gates using an ancilla photon, linear optical elements, and quantum non-demolition (QND) detectors based on weak XKNLs, X-homodyne detectors, and feed-forwards.[56] This indicates that controlled gates can be experimentally realized by the weak XKNL with a large amplitude of the probe beam in coherent state. In 2009, Lin *et al.* presented an almost deterministic controlled-path (C-path) gate and probabilistic controlled gates, such as controlled-σ_X (CNOT), Fredkin, Toffoli, and arbitrary CU gates, using the coherent states, XKNLs, and no ancilla photon.[57] Thereafter, similar schemes for implementing photonic gates were developed.[58–64] Quantum communications and quantum entanglement based on the implementation of CU gates via weak XKNLs[58–62] have been also investigated.

In this paper, for the first time, we propose a deterministic and experimentally feasible CU gate, which is composed of the consecutive operation of a C-path gate and a gathering-path (G-path) gate via weak XKNLs, X-homodyne detectors, and feed-forwards. Subsequently, we present a BQTP scheme, in which Alice and Bob simultaneously teleport their unknown photon states by transmitting only one photon, using linear optical devices and CU gates. This bidirectional quantum communication scheme was developed based on unidirectional quantum communication[45] (using intra-particle hybrid entanglement) and UQTP, which utilizes deterministic Bell-state measurements via XKNLs[34] and optical cavities[35] that use inter-particle hyperentanglement. This paper is organized as follows. In Section 2, we propose a CU gate performed by the consecutive operation of a C-path gate[57] and a G-path gate via XKNLs, X-homodyne detectors, and feed-forwards. Furthermore, we demonstrate that this gate is almost deterministic and experimentally feasible if we choose weak XKNLs and a large amplitude of the coherent states. In Section 3, we present a BQTP scheme that simultaneously teleports two unknown photons between Alice and Bob. In this scheme, we directly transmit only one photon T, which is entangled between the path and polarization (path-polarization intra-particle hybrid entanglement), and use optical elements, such as beam splitters (BSs), polarizing beam splitters (PBSs), spin flippers (SFs), wavelength plates (WPs), polarizing detectors (PDs), and CU (two CNOT, a CZ: controlled-σ_Z, and a CY: controlled-iσ_Y) operations by CU gates, as described in Section 2. Finally, we discuss the success probability and experimental implementation of the proposed CU gate and BQTP in Section 4.

2. Controlled-unitary (CU) gate with cross-Kerr nonlinearity (XKNL)

Let us consider two types of photon polarization: linear-polarization ($|H\rangle$ is horizontal and $|V\rangle$ is vertical) and circular-polarization ($|R\rangle$ is right- and $|L\rangle$ is left-circular). The relationships between the two types are given by

$$|H\rangle \equiv |0\rangle = \frac{1}{\sqrt{2}}\left(|R\rangle + |L\rangle\right), \quad |V\rangle \equiv |1\rangle = \frac{1}{\sqrt{2}}\left(|R\rangle - |L\rangle\right),$$
$$|R\rangle \equiv |+\rangle = \frac{1}{\sqrt{2}}\left(|H\rangle + |V\rangle\right), \quad |L\rangle \equiv |-\rangle = \frac{1}{\sqrt{2}}\left(|H\rangle - |V\rangle\right). \quad (1)$$

Thus, the linearly polarized states correspond to the eigenstates of σ_Z : $\{|H\rangle \equiv |0\rangle, |V\rangle \equiv |1\rangle\}$ and the circularly polarized states to the eigenstates of σ_X : $\{|R\rangle \equiv |+\rangle, |L\rangle \equiv |-\rangle\}$. In order to explain the CU gate, we introduce the XKNL. The Hamiltonian of the XKNL is given by

$$H_{\text{Kerr}} = \hbar\chi N_1 N_2, \quad (2)$$

where N_i is the photon number operator and χ is the strength of nonlinearity of the Kerr-medium. Let us assume that $|n\rangle_i$ represents a state of n photons (signal), and the probe beam is in a coherent state $|\alpha\rangle_j$. After passing through the Kerr-medium, the state of the signal-probe system is given by

$$U_{\text{Kerr}}|n\rangle_1|\alpha\rangle_2 = \mathrm{e}^{\mathrm{i}\theta N_1 N_2}|n\rangle_1|\alpha\rangle_2 = |n\rangle_1\left|\alpha\,\mathrm{e}^{\mathrm{i}n\theta}\right\rangle_2, \quad (3)$$

where $\theta = \chi t$ and t is the interaction time. During this interaction, the signal photon is unaffected, and the phase of the probe beam $|\alpha\rangle_2$ is shifted to $\left|\alpha\,\mathrm{e}^{\mathrm{i}n\theta}\right\rangle_2$ according to the number of photons n in the state $|n\rangle_1$.

Now, we propose a deterministic CU gate that is composed of consecutively performing C-path[57] and G-path gates, an arbitrary unitary operator U, XKNLs, X-homodyne detectors, feed-forwards, and linear optical elements, such as PBSs and BSs, as shown in Fig. 1. Suppose that the initial state of two photons is

$$|\varphi\rangle_{\text{int}} = \alpha|H\rangle_{\text{c}}^1|H\rangle_{\text{t}}^3 + \beta|H\rangle_{\text{c}}^1|V\rangle_{\text{t}}^3 + \gamma|V\rangle_{\text{c}}^1|H\rangle_{\text{t}}^3 + \delta|V\rangle_{\text{c}}^1|V\rangle_{\text{t}}^3, \quad (4)$$

where the superscripts describe photon paths, and the subscripts c and t represent the control and target photon, respectively.

In the C-path gate,[57] as shown in Fig. 1, both the control photon c and target photon t pass through a PBS and a BS. When passing through the PBS, $|H\rangle$ is transmitted and $|V\rangle$ is reflected. The action of 50:50 BS is described by

$$a_{\text{U}}^{+} \to \frac{1}{\sqrt{2}}\left(a_{\text{U}}^{+} + a_{\text{D}}^{+}\right), \quad a_{\text{D}}^{+} \to \frac{1}{\sqrt{2}}\left(a_{\text{U}}^{+} - a_{\text{D}}^{+}\right), \quad (5)$$

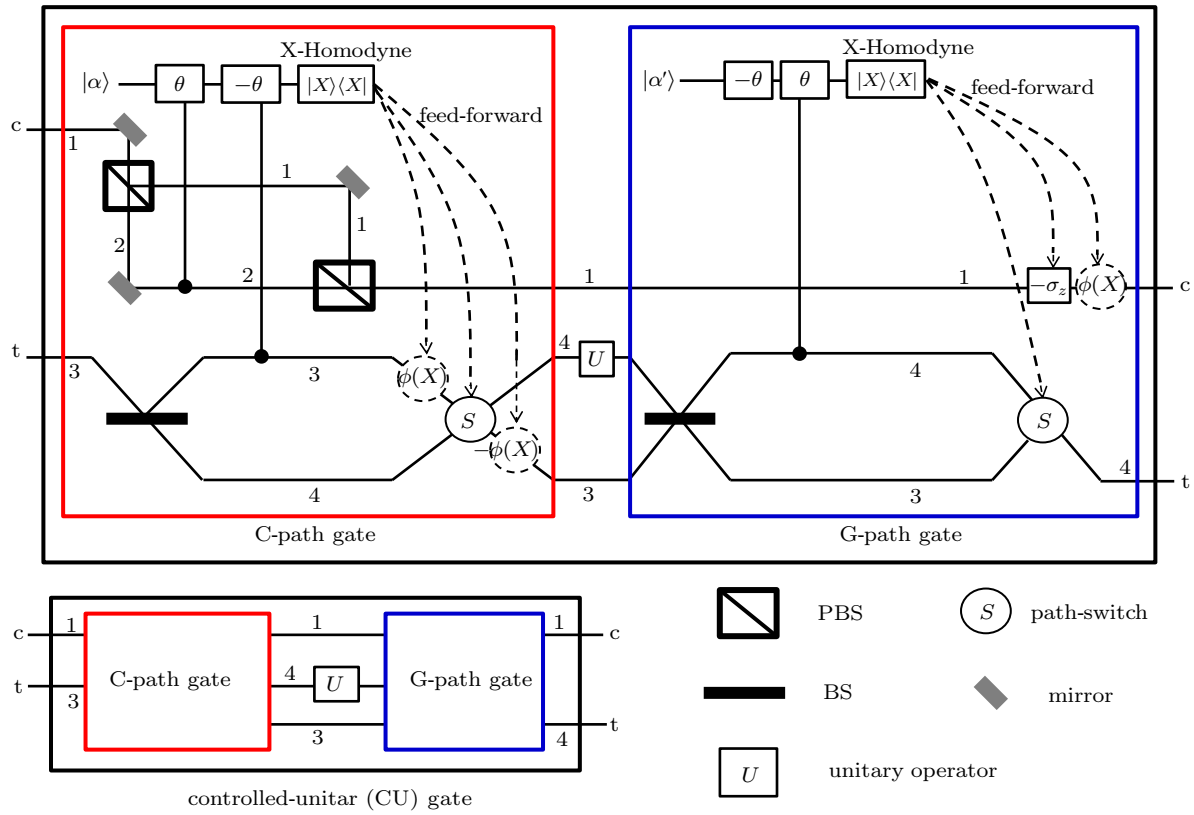


Fig. 1. (color online) The CU gate (black box) is comprised of the consecutive operation of a C-path gate (red box) and a G-path gate (blue box) using XKNLs, X-homodyne detectors, and feed-forwards. The CU gate is composed of three parts, the C-path gate, U operator, and G-path gate. First, in the C-path gate,[57] the two photons (c and t) in the input state induce the controlled phase shifts θ and $-\theta$ in the probe beam (coherent state: $|\alpha\rangle$) by the interaction of XKNLs. Then, we measure the coherent state with the X-homodyne detector, $|X\rangle\langle X|$, which can discriminate the coherent state $|\alpha\rangle$ from the other coherent states, $\left|\alpha e^{+i\theta}\right\rangle$ and $\left|\alpha e^{-i\theta}\right\rangle$. According to the measurement outcome X of the X-homodyne detector, we determine whether or not to operate the phase shifters ($\phi(X)$, $-\phi(X)$) and the path-switch S on the target photon t by feed-forward. After passing the C-path gate, the path of the target photon is split according to the polarization of the control photon. The target photon goes through path 3 (or 4) when the control photon is $|H\rangle$ (or $|V\rangle$). In the second step, the unitary operator U on path 4 is applied to the target photon. In the third step of the G-path gate, the XKNLs induce a phase shift $-\theta$ and θ in the probe beam in the coherent state $|\alpha'\rangle$ according to the photons c and t. To gather the target photon on the split-path, we finally apply the unitary operator $-\sigma_Z$ and the phase shifter $\phi(X)$ to the control photon, and the path-switch S to the target photon via the feed-forward, depending on the measurement outcome of the X-homodyne detector on the probe beam. Consequently, the CU gate performs a controlled-unitary operation on the input state.

where a_i^+ is a creation operator of a photon on path i (U is an up path and D is a down path). After the interaction of the XKNLs between the two photons (c and t) and with the probe beam in a coherent state $|\alpha\rangle$, the control photon passes through a PBS. By the interaction of XKNLs, the control photon c induces a controlled phase shift θ in the probe beam $|\alpha\rangle$ and the target photon t induces a controlled phase shift $-\theta$ in $|\alpha\rangle$, as described in Eq. (3). Then, the photon state is transformed to $|\varphi\rangle_{\rm CP}$ given by

$$\begin{aligned}|\varphi\rangle_{\rm CP} = & \frac{1}{\sqrt{2}}\Big(\alpha|H\rangle_{\rm c}^1|H\rangle_{\rm t}^3+\beta|H\rangle_{\rm c}^1|V\rangle_{\rm t}^3+\gamma|V\rangle_{\rm c}^1|H\rangle_{\rm t}^4 \\ & +\delta|V\rangle_{\rm c}^1|V\rangle_{\rm t}^4\Big)|\alpha\rangle \\ & +\frac{1}{\sqrt{2}}\Big(\alpha|H\rangle_{\rm c}^1|H\rangle_{\rm t}^4+\beta|H\rangle_{\rm c}^1|V\rangle_{\rm t}^4\Big)|\alpha e^{i\theta}\rangle \\ & +\frac{1}{\sqrt{2}}\Big(\gamma|V\rangle_{\rm c}^1|H\rangle_{\rm t}^3+\delta|V\rangle_{\rm c}^1|V\rangle_{\rm t}^3\Big)|\alpha e^{-i\theta}\rangle. \quad (6)\end{aligned}$$

The probe beam in the coherent state is then measured by an X-homodyne detector, which cannot distinguish the states $|\alpha e^{-i\theta}\rangle$ from $|\alpha e^{+i\theta}\rangle$, but does discriminate $|\alpha\rangle$ from $|\alpha e^{+i\theta}\rangle$ (or $|\alpha e^{-i\theta}\rangle$). If no phase shift is induced in the coherent state $|\alpha\rangle$, then the collapsed state $|\varphi\rangle_\alpha$ is given by

$$|\varphi\rangle_\alpha = \alpha|H\rangle_{\rm c}^1|H\rangle_{\rm t}^3+\beta|H\rangle_{\rm c}^1|V\rangle_{\rm t}^3+\gamma|V\rangle_{\rm c}^1|H\rangle_{\rm t}^4+\delta|V\rangle_{\rm c}^1|V\rangle_{\rm t}^4. \quad (7)$$

If a phase shift is induced in the coherent state $|\alpha e^{\pm i\theta}\rangle$, then the phase shifters ($\phi(X)$, $-\phi(X)$) and path-switch S may be applied to the target photon through feed-forward, depending on the measurement result X. Consequently, the final state will be the same as the state $|\varphi\rangle_\alpha$. This C-path gate, using weak XKNLs and a strong coherent state, is nearly deterministic with a certain success probability ($P_{\rm succ}^{\rm CP}=1$), as mentioned in Ref. [57]. After passing the C-path, the path of the target photon is split, as shown in Eq. (7).

In the second step, the target photon in the state $|\varphi\rangle_\alpha$ passes through an arbitrary unitary operator U on path 4. The

transformed state $|\varphi\rangle_{\rm U}$ is represented as

$$\begin{aligned}|\varphi\rangle_{\rm U} &= (U)_{\rm t}^4 |\phi\rangle_\alpha \\ &= \alpha |H\rangle_{\rm c}^1 |H\rangle_{\rm t}^3 + \beta |H\rangle_{\rm c}^1 |V\rangle_{\rm t}^3 + \gamma |V\rangle_{\rm c}^1 \left(U|H\rangle_{\rm t}^4\right) \\ &\quad + \delta |V\rangle_{\rm c}^1 \left(U|V\rangle_{\rm t}^4\right). \end{aligned} \tag{8}$$

For example, if U is σ_X, σ_Z, or $\mathrm{i}\sigma_Y$, then the state $|\varphi\rangle_{\rm U}$ will be given by

$$\begin{aligned}|\varphi\rangle_{\sigma_X} &= (\sigma_X)_{\rm t}^4 |\varphi\rangle_\alpha \\ &= \alpha |H\rangle_{\rm c}^1 |H\rangle_{\rm t}^3 + \beta |H\rangle_{\rm c}^1 |V\rangle_{\rm t}^3 + \gamma |V\rangle_{\rm c}^1 |V\rangle_{\rm t}^4 + \delta |V\rangle_{\rm c}^1 |H\rangle_{\rm t}^4, \\ |\varphi\rangle_{\sigma_Z} &= (\sigma_Z)_{\rm t}^4 |\varphi\rangle_\alpha \\ &= \alpha |H\rangle_{\rm c}^1 |H\rangle_{\rm t}^3 + \beta |H\rangle_{\rm c}^1 |V\rangle_{\rm t}^3 + \gamma |V\rangle_{\rm c}^1 |H\rangle_{\rm t}^4 - \delta |V\rangle_{\rm c}^1 |V\rangle_{\rm t}^4, \\ |\varphi\rangle_{\mathrm{i}\sigma_Y} &= (\mathrm{i}\sigma_Y)_{\rm t}^4 |\varphi\rangle_\alpha \\ &= \alpha |H\rangle_{\rm c}^1 |H\rangle_{\rm t}^3 + \beta |H\rangle_{\rm c}^1 |V\rangle_{\rm t}^3 - \gamma |V\rangle_{\rm c}^1 |V\rangle_{\rm t}^4 \\ &\quad + \delta |V\rangle_{\rm c}^1 |H\rangle_{\rm t}^4. \end{aligned} \tag{9}$$

These are the output states of the unitary operation of CNOT, CZ, or CY on the initial state of the two photons (Eq. (4)), respectively. Since the path of the target photon is divided into two paths, 3 and 4, in Eq. (9), we use the G-path gate to merge the split-path of the target photon into a single path.

In the G-path gate of the third step, as described in Fig. 1, the target photon in $|\varphi\rangle_{\rm U}$ passes through a BS. By the interaction of XKNLs, the control photon c induces a controlled phase shift $-\theta$, and the target photon t induces a controlled phase shift θ in the probe beam in the coherent state $|\alpha'\rangle$, as in Eq. (3). Then, the transformed state $|\varphi\rangle_{\rm GP}$ is given by

$$\begin{aligned}|\varphi\rangle_{\rm GP} &= \frac{1}{\sqrt{2}}\Big[\alpha |H\rangle_{\rm c}^1 |H\rangle_{\rm t}^4 + \beta |H\rangle_{\rm c}^1 |V\rangle_{\rm t}^4 + \gamma |V\rangle_{\rm c}^1 \left(U|H\rangle_{\rm t}^4\right) \\ &\quad + \delta |V\rangle_{\rm c}^1 \left(U|V\rangle_{\rm t}^4\right)\Big] |\alpha'\rangle \\ &\quad + \frac{1}{\sqrt{2}}\Big[-\alpha |H\rangle_{\rm c}^1 |H\rangle_{\rm t}^3 - \beta |H\rangle_{\rm c}^1 |V\rangle_{\rm t}^3 + \gamma |V\rangle_{\rm c}^1 \left(U|H\rangle_{\rm t}^3\right) \\ &\quad + \delta |V\rangle_{\rm c}^1 \left(U|V\rangle_{\rm t}^3\right)\Big] \left|\alpha' \mathrm{e}^{-\mathrm{i}\theta}\right\rangle. \end{aligned} \tag{10}$$

In Eq. (10), unlike Eq. (9), the path of the target photon and the phase state of the coherent probe beam are entangled with each other. Subsequently, the X-homodyne detector[59] measures the probe beam in the coherent state. When α' is real, the projection of $|\varphi\rangle_{\rm GP}$ onto an eigenstate $|X\rangle$ of the observable X is given by

$$\begin{aligned}|\varphi\rangle_X &= \langle X|\varphi\rangle_{\rm GP} \\ &= \frac{1}{\sqrt{2}} f(X,\alpha') \Big[\alpha |H\rangle_{\rm c}^1 |H\rangle_{\rm t}^4 + \beta |H\rangle_{\rm c}^1 |V\rangle_{\rm t}^4 \\ &\quad + \gamma |V\rangle_{\rm c}^1 \left(U|H\rangle_{\rm t}^4\right) + \delta |V\rangle_{\rm c}^1 \left(U|V\rangle_{\rm t}^4\right)\Big] \\ &\quad + \frac{1}{\sqrt{2}} f(X,\alpha'\cos\theta)\, \mathrm{e}^{-\mathrm{i}\phi(X)} \Big[-\alpha |H\rangle_{\rm c}^1 |H\rangle_{\rm t}^3 \\ &\quad - \beta |H\rangle_{\rm c}^1 |V\rangle_{\rm t}^3 + \gamma |V\rangle_{\rm c}^1 \left(U|H\rangle_{\rm t}^3\right) \\ &\quad + \delta |V\rangle_{\rm c}^1 \left(U|V\rangle_{\rm t}^3\right)\Big], \end{aligned} \tag{11}$$

where we use[65]

$$\begin{aligned}\left\langle X|\alpha' \mathrm{e}^{\pm\mathrm{i}\theta}\right\rangle &= \frac{1}{\sqrt[4]{2\pi}} \exp\Big[\frac{-1}{4}(X - 2\alpha'\cos\theta)^2 \\ &\quad \pm \mathrm{i}\left\{\alpha'\sin\theta\left(X - \alpha'\cos\theta\right)\right\}\Big], \\ f(X,\omega) &= \frac{1}{\sqrt[4]{2\pi}} \exp\Big[\frac{-1}{4}(X - 2\omega)^2\Big], \\ \phi(X) &= \alpha'\sin\theta\left(X - \alpha'\cos\theta\right)[\mathrm{mod}\, 2\pi]. \end{aligned} \tag{12}$$

As shown in Eq. (12), the square of $f(X,\alpha')$ or $f(X,\alpha'\cos\theta)$ in Eq. (11) is a Gaussian distribution. The Gaussian curves have peaks at $2\alpha'$ and $2\alpha'\cos\theta$, and the midpoint of the two peaks is $X_0 = \alpha'(1+\cos\theta)$, as shown in Fig. 2. When the distance $X_{\rm d}$ between these peaks is sufficiently large, there is little overlap between the two curves and it is possible to distinguish $|\alpha'\rangle$ from $\left|\alpha' \mathrm{e}^{-\mathrm{i}\theta}\right\rangle$ with a nearly certain probability by an X-homodyne measurement. For example, if we obtain the measurement result X, which is larger than X_0, we can construe the state of the two photons c and t as

$$\begin{aligned}|\varphi\rangle_{X>X_0} &= \alpha |H\rangle_{\rm c}^1 |H\rangle_{\rm t}^4 + \beta |H\rangle_{\rm c}^1 |V\rangle_{\rm t}^4 \\ &\quad + \gamma |V\rangle_{\rm c}^1 \left(U|H\rangle_{\rm t}^4\right) + \delta |V\rangle_{\rm c}^1 \left(U|V\rangle_{\rm t}^4\right). \end{aligned} \tag{13}$$

The state $|\varphi\rangle_{X>X_0}$ is the output of the CU operations in the C- and G-path gates on the initial state $|\varphi\rangle_{\rm int}$ of the two photons of Eq. (4). The target photon in the state $|\varphi\rangle_{X>X_0}$ is in the single path 4. This means that the split-path of the target photon in Eq. (8) is merged to the single path 4 by the G-path gate. If the measurement result X is smaller than X_0, then the state of the two photons (c, t) will be

$$\begin{aligned}|\varphi\rangle_{X<X_0} &= \mathrm{e}^{-\mathrm{i}\phi(X)}\Big[-\alpha |H\rangle_{\rm c}^1 |H\rangle_{\rm t}^3 - \beta |H\rangle_{\rm c}^1 |V\rangle_{\rm t}^3 \\ &\quad + \gamma |V\rangle_{\rm c}^1 \left(U|H\rangle_{\rm t}^3\right) + \delta |V\rangle_{\rm c}^1 \left(U|V\rangle_{\rm t}^3\right)\Big]. \end{aligned} \tag{14}$$

Subsequently, according to the feed-forward, which depends on the measurement result X, a $-\sigma_z$ operation and a phase shifter $\phi(X)$ are performed on the control photon c, and the path-switch S can change the path of the target photon t from path 3 to path 4. The final state $|\varphi\rangle_{\rm fin}$ will be

$$\begin{aligned}|\varphi\rangle_{X<X_0} \xrightarrow{\text{feed-forward}} |\varphi\rangle_{\rm fin} &= \alpha |H\rangle_{\rm c}^1 |H\rangle_{\rm t}^4 + \beta |H\rangle_{\rm c}^1 |V\rangle_{\rm t}^4 \\ &\quad + \gamma |V\rangle_{\rm c}^1 \left(U|H\rangle_{\rm t}^4\right) \\ &\quad + \delta |V\rangle_{\rm c}^1 \left(U|V\rangle_{\rm t}^4\right), \end{aligned} \tag{15}$$

where the state $|\varphi\rangle_{\rm fin}$ is the same as the state $|\varphi\rangle_{X>X_0}$ in Eq. (13). Consequently, the state $|\varphi\rangle_{X<X_0}$ is converted to the state $|\varphi\rangle_{X>X_0}$, which is the output of the CU operation on the initial state $|\varphi\rangle_{\rm int}$ of the two photons in Eq. (4) using feed-forward.

For the nearly deterministic CU gate, which is composed of the consecutive operation of the C- and G-path gates, the

overlap between the two curves, $f(X,\alpha')$ and $f(X,\alpha'\cos\theta)$, in the G-path gate should be small. This means that the two coherent states $|\alpha'\rangle$ and $\left|\alpha' e^{-i\theta}\right\rangle$ are deterministically distinguishable by an X-homodyne measurement. We can obtain the error probability of the G-path gate with the same method as that in Ref. [64]. The small overlap between the two Gaussian curves allows the calculation of the error probability, which is determined as follows:

$$P_{\text{error}}^{\text{GP}} = \frac{1}{2}\left[1-\text{erf}\left(\frac{X_{\text{d}}}{2\sqrt{2}}\right)\right], \tag{16}$$

where $\text{erf}(x)$ is a Gauss error function and X_{d} is the distance between the two peaks, as shown in Fig. 2. $P_{\text{error}}^{\text{GP}}$ is smaller than 10^{-5} when $X_{\text{d}} = 2\alpha'(1-\cos\theta) \sim \alpha'\theta^2 > 9$. This indicates that if we can choose the amplitude α' of the probe beam to be sufficiently large, then the weak XKNL ($\theta \ll 1$) can also be utilized for the G-path gate. Consequently, the CU gate can be composed of the consecutive operations of the C- and G-path gates, and its probabilities ($P_{\text{succ}}^{\text{CP}}$, $P_{\text{succ}}^{\text{GP}}$) of success for the C-path[57] and G-path gate approach 1 when strong coherent states and weak XKNLs are employed. Thus, this CU gate is nearly deterministic. Furthermore, the XKNL is not necessarily very large because it can be compensated by using a coherent state with very large amplitude. Owing to the use of weak XKNLs, the proposed CU gate is potentially available for experimental implementation.

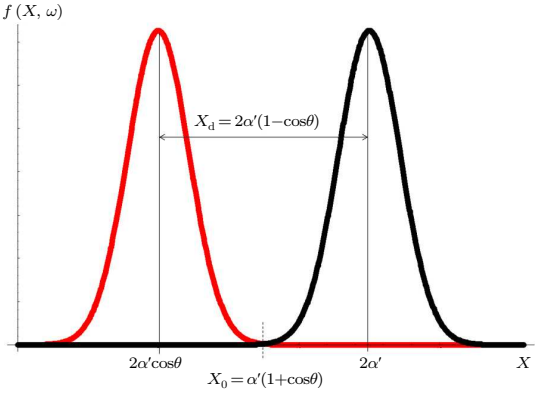


Fig. 2. (color online) Gaussian probability distribution of the measurements of the probe beam in a coherent state, acquired by an X-homodyne measurement: the black and red curves correspond to $f(X,\alpha')$ and $f(X,\alpha'\cos\theta)$, respectively. X_0 is the midpoint of the two peaks and X_{d} is the distance between them.

3. BQTP using intra-particle hybrid entanglement and CU gates

Figure 3 shows the configuration of the BQTP for the simultaneous teleportation of the unknown photon states between Alice and Bob using intra-particle hybrid entanglement, linear optical elements, and CU operations (by CU gates), which are composed of consecutive operations of C-path and G-path gates, as described in Section 2. Let us assume the two unknown states $|\psi\rangle_{\text{A}}$ and $|\varphi\rangle_{\text{B}}$ of photons A and B, respectively, which Alice and Bob want to teleport to each other

$$|\psi\rangle_{\text{A}} = \alpha|H\rangle_{\text{A}} + \beta|V\rangle_{\text{A}}, \quad |\varphi\rangle_{\text{B}} = \chi|H\rangle_{\text{B}} + \delta|V\rangle_{\text{B}}, \tag{17}$$

where $|\alpha|^2+|\beta|^2 = |\chi|^2+|\delta|^2 = 1$. For simultaneous teleportation, Alice prepares the transmission photon T in the horizontal polarization state $|H\rangle_{\text{T}}$ and sends it to Bob along path P. This initial photon state $|\Phi\rangle_{\text{int}}$ is given by

$$|\Phi\rangle_{\text{int}} = |H\rangle_{\text{T}}^{\text{P}}. \tag{18}$$

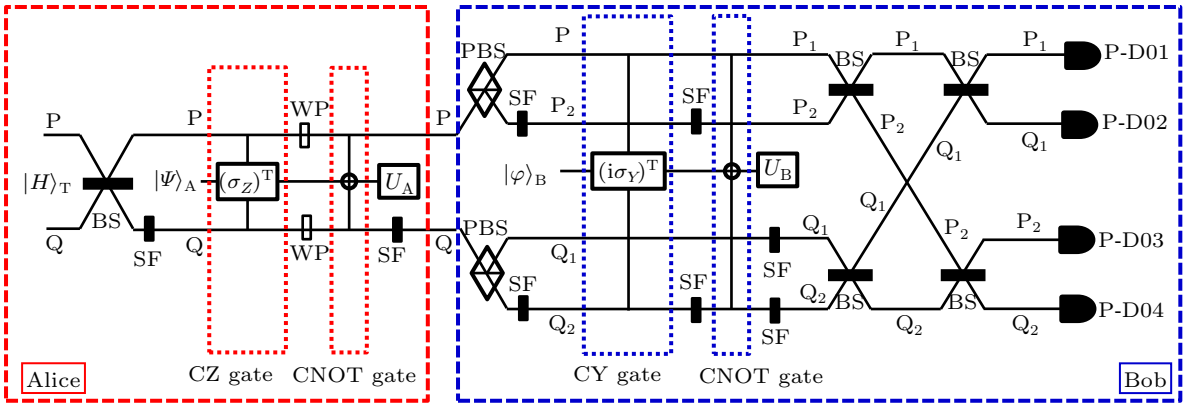


Fig. 3. (color online) Schematic diagram of the BQTP scheme between Alice and Bob using intra-particle hybrid entanglement and CU gates: Alice wants to teleport an unknown state $|\psi\rangle_{\text{A}}$ of photon A to Bob, and Bob wants to teleport an unknown state $|\varphi\rangle_{\text{B}}$ of photon B to Alice. To implement our simultaneous teleportation scheme, Alice prepares the transmission photon $|H\rangle_{\text{T}}$ and generates photon T to the path-polarization intra-particle hybrid entangled state using a BS and an SF. After performing a CZ and a CNOT gate between the two photons T and A ($|\psi\rangle_{\text{A}}$), Alice transfers photon T to Bob. Subsequently, Bob performs a CY and CNOT gate between the two photons T and B for the teleportation of his unknown photon state $|\varphi\rangle_{\text{B}}$ to Alice. Consequently, Alice and Bob can simultaneously teleport the unknown states $|\psi\rangle_{\text{A}}$ and $|\varphi\rangle_{\text{B}}$ to each other through BSs, PBSs, SFs, WPs, and CU operations (Alice's side: a CZ gate and a CNOT gate, Bob's side: a CY gate and CNOT gate). Then, Bob measures the path and polarization of the transmitted photon T through P-Ds (01-04). These measurement results and the information on the initial path of photon T are shared through a classical channel in order to reconstruct the teleported states of photons to obtain the initial unknown photon states, $|\psi\rangle_{\text{A}}$and $|\varphi\rangle_{\text{B}}$, by applying the appropriate unitary operators U_{A} and U_{B}. Consequently, Alice and Bob achieve simultaneous teleportation by transmitting only a single photon T, in which the states of photons A and B are converted to the unknown states $|\varphi\rangle_{\text{B}}$ and $|\psi\rangle_{\text{A}}$ of Bob and Alice, respectively.

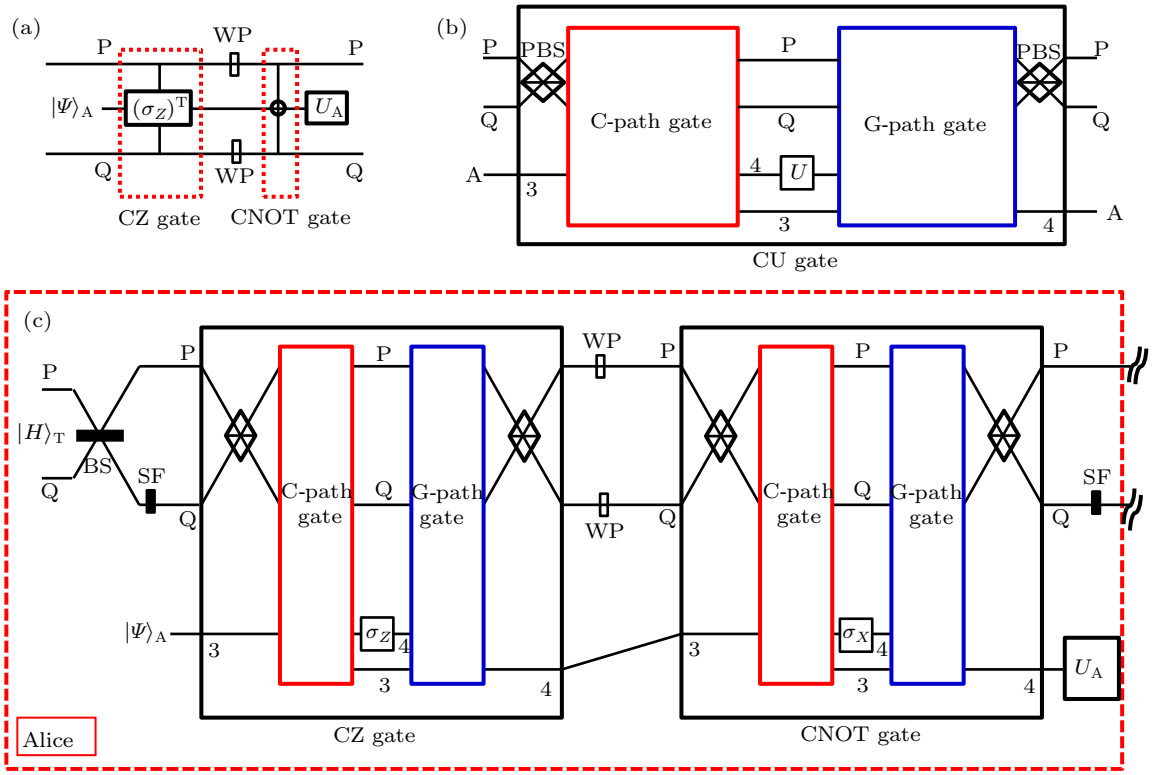


Fig. 4. (color online) (a) Alice's side in Fig. 3, when the CU (CZ, CNOT) operations are performed between the control photon T (the transmission photon) and the target photon A (Alice's unknown state $|\psi\rangle_A$). (b) Schematic illustration of the CU gate, in which the C-path and G-path gates are consecutively performed by XKNLs, X-homodyne detectors, and feed-forwards, as described in Section 2. If the unitary operator U in the middle between the C-path and G-path gates is σ_Z or σ_X, then the CU gate will become a CZ gate or a CNOT gate. The PBS in front of the C-path gate and the PBS at the rear of the G-path gate in path P–Q refer to the split-path of control photon T. The details are presented in Appendix A. (c) A detailed description of the operations on Alice's side, using a CZ gate and CNOT gate (the consecutive operation of a C-path gate and a G-path gate) via XKNLs, X-homodyne detectors, and feed-forwards.

Figure 4(c) shows a detailed description of the operations on Alice's side. After the initial photon state $|\Phi\rangle_{\text{int}}$ passes through a BS and an SF on path Q, it is transformed to a path-polarization intra-particle hybrid entangled state $|\Phi\rangle_1$ given by

$$|\Phi\rangle_1 = \frac{1}{\sqrt{2}}\left(|H\rangle_T^P + |V\rangle_T^Q\right), \tag{19}$$

where the SF flips the linear polarization of the photon state, $|H\rangle \to |V\rangle, |V\rangle \to |H\rangle$ ($U_{SF} = |H\rangle\langle V| + |V\rangle\langle H|$). Subsequently, Alice performs the CZ gate, in which the state $|\Phi\rangle_1$ is used as the control photon, and the unknown photon $|\psi\rangle_A$ of Eq. (17), which would be teleported from Alice to Bob, is used as the target photon. Then the polarizations of photon T are converted by two WPs, which are similar to the Hadamard operator, ($|H\rangle \to |R\rangle, |V\rangle \to |L\rangle$), along paths P and Q. After Alice performs the CNOT gate, in which the state of photon T is used as the control photon and photon A is used as the target photon, photon T passes through the SF on path Q. Consequently, Alice's final state $|\Phi\rangle_{\text{Alice}}$ is given by

$$\begin{aligned}|\Phi\rangle_1 &\xrightarrow{\text{CZ gate (photons T–A)}} \frac{1}{\sqrt{2}}\Big[|H\rangle_T^P(\alpha|H\rangle_A + \beta|V\rangle_A) \\ &\quad + |V\rangle_T^Q(\alpha|H\rangle_A - \beta|V\rangle_A)\Big] \\ &\xrightarrow{\text{WP (path P, Q)}} \frac{1}{\sqrt{2}}\Big[|R\rangle_T^P(\alpha|H\rangle_A + \beta|V\rangle_A) \\ &\quad + |L\rangle_T^Q(\alpha|H\rangle_A - \beta|V\rangle_A)\Big] \\ &\xrightarrow{\text{CNOT gate (photons T–A), SF (path Q)}} \\ |\Phi\rangle_{\text{Alice}} &= \frac{1}{2}\Big[|H\rangle_T^P(\alpha|H\rangle_A + \beta|V\rangle_A) \\ &\quad + |V\rangle_T^P(\alpha|V\rangle_A + \beta|H\rangle_A) \\ &\quad - |H\rangle_T^Q(\alpha|V\rangle_A - \beta|H\rangle_A) \\ &\quad + |V\rangle_T^Q(\alpha|H\rangle_A - \beta|V\rangle_A)\Big],\end{aligned} \tag{20}$$

where the CZ and CNOT gates on Alice's side are described in Appendix A. Only photon T is directly transmitted and photon A in the final state $|\Phi\rangle_{\text{Alice}}$ remains with Alice.

Figure 5(c) shows a detailed description of the operations on Bob's side. After Bob receives photon T in state $|\Phi\rangle_{\text{Alice}}$, he transmits it through the PBSs along paths P and Q. It then passes through the SFs along paths P_2 and Q_2. Subsequently, Bob performs the CY gate, in which the state of photon T is used as the control photon and the unknown photon $|\varphi\rangle_B$ of Eq. (17), which would be teleported from Bob to Alice and used as the target photon. Then, photon T passes through the SFs along paths P_2 and Q_2. Finally, after Bob performs the CNOT gate, in which the state of photon T is used as the control photon and photon B is used as the target photon, photon T passes through the SF on paths Q_1 and Q_2. Consequently,

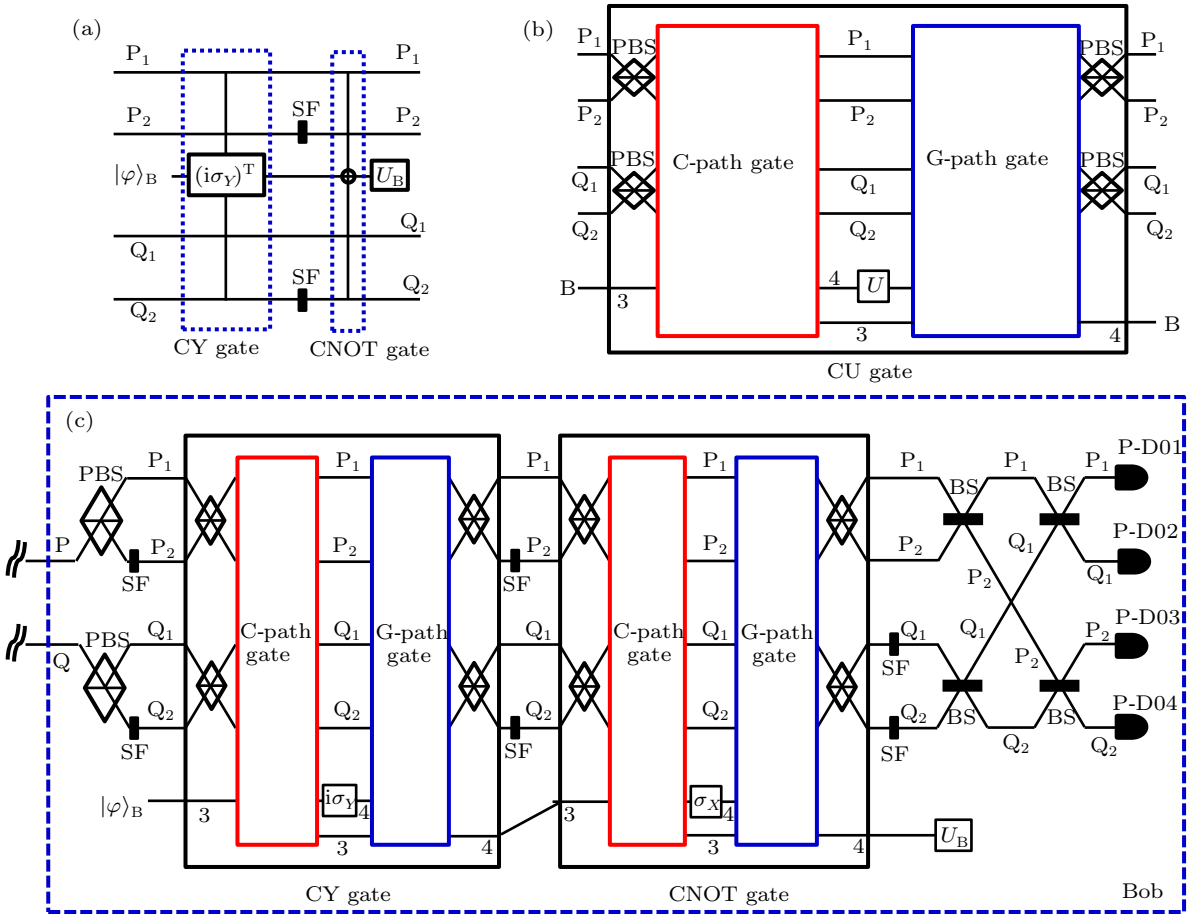


Fig. 5. (color online) (a) Bob's side in Fig. 3, when the CU (CY, CNOT) operations are performed between the control photon T (the transmission photon) and the target photon B (Bob's unknown state $|\varphi\rangle_{\rm B}$). (b) Schematic depiction of the CU gate, in which the C-path gate and the G-path gate are consecutively performed by XKNLs, X-homodyne detectors, and feed-forwards, as described in Section 2. If the unitary operator U in the middle between the C-path gate and the G-path gate is $\mathrm{i}\sigma_Y$ or σ_X, then the CU gate becomes a CY gate or CNOT gate. Furthermore, the PBSs in front of the C-path gate and at the rear of the G-path gate in the paths P_1–P_2 and Q_1–Q_2 refer to the split-path of the control photon T. The details are presented in Appendix B. (c) Detailed description of the operations on Bob's side, using a CY gate and CNOT gate (the consecutive operation of C-path gate and G-path gate) via XKNLs, X-homodyne detectors, and feed-forwards.

the transformed state $|\Psi\rangle_1$ is given by

$$
\begin{aligned}
|\Phi\rangle_{\rm Alice} &\xrightarrow{\text{PBSs (path P, Q), SF (path P}_2\text{, Q}_2\text{)}} \\
&\frac{1}{2}\Big[|H\rangle_{\rm T}^{\rm P_1}(\alpha|H\rangle_{\rm A}+\beta|V\rangle_{\rm A}) \\
&+|H\rangle_{\rm T}^{\rm P_2}(\alpha|V\rangle_{\rm A}+\beta|H\rangle_{\rm A}) \\
&-|V\rangle_{\rm T}^{\rm Q_2}(\alpha|V\rangle_{\rm A}-\beta|H\rangle_{\rm A}) \\
&+|V\rangle_{\rm T}^{\rm Q_1}(\alpha|H\rangle_{\rm A}-\beta|V\rangle_{\rm A})\Big] \\
&\xrightarrow{\text{CY gate (photons T–B), SF (path P}_2\text{, Q}_2\text{)}} \\
&\frac{1}{2}\Big[|H\rangle_{\rm T}^{\rm P_1}(\alpha|H\rangle_{\rm A}+\beta|V\rangle_{\rm A})(\chi|H\rangle_{\rm B}+\delta|V\rangle_{\rm B}) \\
&+|V\rangle_{\rm T}^{\rm P_2}(\alpha|V\rangle_{\rm A}+\beta|H\rangle_{\rm A})(\chi|H\rangle_{\rm B}+\delta|V\rangle_{\rm B}) \\
&+|H\rangle_{\rm T}^{\rm Q_2}(\alpha|V\rangle_{\rm A}-\beta|H\rangle_{\rm A})(\chi|V\rangle_{\rm B}-\delta|H\rangle_{\rm B}) \\
&-|V\rangle_{\rm T}^{\rm Q_1}(\alpha|H\rangle_{\rm A}-\beta|V\rangle_{\rm A})(\chi|H\rangle_{\rm B}-\delta|V\rangle_{\rm B})\Big] \\
&\xrightarrow{\text{CNOT gate (photons T–B), SF (path Q}_1\text{, Q}_2\text{)}} \\
|\Psi\rangle_1 &= \frac{1}{2}\Big[|H\rangle_{\rm T}^{\rm P_1}(\alpha|H\rangle_{\rm A}+\beta|V\rangle_{\rm A})(\chi|H\rangle_{\rm B}+\delta|V\rangle_{\rm B}) \\
&+|V\rangle_{\rm T}^{\rm P_2}(\alpha|V\rangle_{\rm A}+\beta|H\rangle_{\rm A})(\chi|H\rangle_{\rm B}+\delta|V\rangle_{\rm B}) \\
&+|V\rangle_{\rm T}^{\rm Q_2}(\alpha|V\rangle_{\rm A}-\beta|H\rangle_{\rm A})(\chi|V\rangle_{\rm B}-\delta|H\rangle_{\rm B}) \\
&-|H\rangle_{\rm T}^{\rm Q_1}(\alpha|H\rangle_{\rm A}-\beta|V\rangle_{\rm A})(\chi|H\rangle_{\rm B}-\delta|V\rangle_{\rm B})\Big], \qquad (21)
\end{aligned}
$$

where the CY gate and CNOT gate on Bob's side are described in Appendix B. Photon T in the state $|\Psi\rangle_1$ passes through the BSs (path P_1–P_2 and path Q_1–Q_2), and then through the BSs (path P_1–Q_1 and path P_2–Q_2). Finally, the output photon state $|\Psi\rangle_{\text{Bob-P}}$, in which photon T is expressed as the circular-polarization states $|R\rangle_{\rm T}$ and $|L\rangle_{\rm T}$ of Eq. (1), is given by

$$
\begin{aligned}
|\Psi\rangle_1 &\xrightarrow{\text{BSs (path P}_1\text{–P}_2\text{ and path Q}_1\text{–Q}_2\text{)}} \\
&\frac{1}{2\sqrt{2}}\Big[|H\rangle_{\rm T}^{\rm P_1}(\alpha|H\rangle_{\rm A}+\beta|V\rangle_{\rm A})(\chi|H\rangle_{\rm B}+\delta|V\rangle_{\rm B}) \\
&+|V\rangle_{\rm T}^{\rm P_1}(\alpha|V\rangle_{\rm A}+\beta|H\rangle_{\rm A})(\chi|V\rangle_{\rm B}+\delta|H\rangle_{\rm B}) \\
&+|H\rangle_{\rm T}^{\rm P_2}(\alpha|H\rangle_{\rm A}+\beta|V\rangle_{\rm A})(\chi|H\rangle_{\rm B}+\delta|V\rangle_{\rm B}) \\
&-|V\rangle_{\rm T}^{\rm P_2}(\alpha|V\rangle_{\rm A}+\beta|H\rangle_{\rm A})(\chi|V\rangle_{\rm B}+\delta|H\rangle_{\rm B}) \\
&-|H\rangle_{\rm T}^{\rm Q_1}(\alpha|H\rangle_{\rm A}-\beta|V\rangle_{\rm A})(\chi|H\rangle_{\rm B}-\delta|V\rangle_{\rm B}) \\
&+|V\rangle_{\rm T}^{\rm Q_1}(\alpha|V\rangle_{\rm A}-\beta|H\rangle_{\rm A})(\chi|V\rangle_{\rm B}-\delta|H\rangle_{\rm B})
\end{aligned}
$$

$$
\begin{aligned}
&-|H\rangle_{\mathrm{T}}^{\mathrm{Q_2}}(\alpha|H\rangle_{\mathrm{A}}-\beta|V\rangle_{\mathrm{A}})(\chi|H\rangle_{\mathrm{B}}-\delta|V\rangle_{\mathrm{B}})\\
&-|V\rangle_{\mathrm{T}}^{\mathrm{Q_2}}(\alpha|V\rangle_{\mathrm{A}}-\beta|H\rangle_{\mathrm{A}})(\chi|V\rangle_{\mathrm{B}}-\delta|H\rangle_{\mathrm{B}})\Big]\\
&\xrightarrow{\text{BSs (path P}_1\text{–Q}_1\text{ and path P}_2\text{–Q}_2\text{), photon }\ T:\{|H\rangle_{\mathrm{T}},|V\rangle_{\mathrm{T}}\}\Rightarrow\{|R\rangle_{\mathrm{T}},|L\rangle_{\mathrm{T}}\}}
\end{aligned}
$$

$$
\begin{aligned}
|\Psi\rangle_{\text{Bob-P}}=\frac{1}{2\sqrt{2}}\Big[&|R\rangle_{\mathrm{T}}^{\mathrm{P_1}}(\chi|V\rangle_{\mathrm{A}}+\delta|H\rangle_{\mathrm{A}})(\beta|H\rangle_{\mathrm{B}}+\alpha|V\rangle_{\mathrm{B}})\\
&+|L\rangle_{\mathrm{T}}^{\mathrm{P_1}}(\chi|V\rangle_{\mathrm{A}}-\delta|H\rangle_{\mathrm{A}})(\beta|H\rangle_{\mathrm{B}}-\alpha|V\rangle_{\mathrm{B}})\\
&+|R\rangle_{\mathrm{T}}^{\mathrm{Q_1}}(\chi|H\rangle_{\mathrm{A}}+\delta|V\rangle_{\mathrm{A}})(\alpha|H\rangle_{\mathrm{B}}+\beta|V\rangle_{\mathrm{B}})\\
&+|L\rangle_{\mathrm{T}}^{\mathrm{Q_1}}(\chi|H\rangle_{\mathrm{A}}-\delta|V\rangle_{\mathrm{A}})(\alpha|H\rangle_{\mathrm{B}}-\beta|V\rangle_{\mathrm{B}})\\
&+|R\rangle_{\mathrm{T}}^{\mathrm{P_2}}(\chi|V\rangle_{\mathrm{A}}-\delta|H\rangle_{\mathrm{A}})(\beta|H\rangle_{\mathrm{B}}-\alpha|V\rangle_{\mathrm{B}})\\
&+|L\rangle_{\mathrm{T}}^{\mathrm{P_2}}(\chi|V\rangle_{\mathrm{A}}+\delta|H\rangle_{\mathrm{A}})(\beta|H\rangle_{\mathrm{B}}+\alpha|V\rangle_{\mathrm{B}})\\
&+|R\rangle_{\mathrm{T}}^{\mathrm{Q_2}}(\chi|H\rangle_{\mathrm{A}}-\delta|V\rangle_{\mathrm{A}})(\alpha|H\rangle_{\mathrm{B}}-\beta|V\rangle_{\mathrm{B}})\\
&+|L\rangle_{\mathrm{T}}^{\mathrm{Q_2}}(\chi|H\rangle_{\mathrm{A}}+\delta|V\rangle_{\mathrm{A}})(\alpha|H\rangle_{\mathrm{B}}+\beta|V\rangle_{\mathrm{B}})\Big].
\end{aligned}
\tag{22}
$$

If Alice sends photon $T(|H\rangle_{\mathrm{T}})$ to Bob along path Q, $|H\rangle_{\mathrm{T}}^{\mathrm{Q}}$, and Alice (Bob) wants to simultaneously teleport an unknown photon $|\psi\rangle_{\mathrm{A}}=\alpha|H\rangle_{\mathrm{A}}+\beta|V\rangle_{\mathrm{A}}$ ($|\varphi\rangle_{\mathrm{B}}=\chi|H\rangle_{\mathrm{B}}+\delta|V\rangle_{\mathrm{B}}$) to Bob (Alice), then the output photon state $|\Psi\rangle_{\text{Bob-Q}}$ is expressed as follows:

$$
\begin{aligned}
|\Psi\rangle_{\text{Bob-Q}}=\frac{1}{2\sqrt{2}}\Big[&|R\rangle_{\mathrm{T}}^{\mathrm{P_1}}(\chi|H\rangle_{\mathrm{A}}+\delta|V\rangle_{\mathrm{A}})(\alpha|H\rangle_{\mathrm{B}}+\beta|V\rangle_{\mathrm{B}})\\
&+|L\rangle_{\mathrm{T}}^{\mathrm{P_1}}(\chi|H\rangle_{\mathrm{A}}-\delta|V\rangle_{\mathrm{A}})(\alpha|H\rangle_{\mathrm{B}}-\beta|V\rangle_{\mathrm{B}})\\
&+|R\rangle_{\mathrm{T}}^{\mathrm{Q_1}}(\chi|V\rangle_{\mathrm{A}}+\delta|H\rangle_{\mathrm{A}})(\beta|H\rangle_{\mathrm{B}}+\alpha|V\rangle_{\mathrm{B}})\\
&+|L\rangle_{\mathrm{T}}^{\mathrm{Q_1}}(\chi|V\rangle_{\mathrm{A}}-\delta|H\rangle_{\mathrm{A}})(\beta|H\rangle_{\mathrm{B}}-\alpha|V\rangle_{\mathrm{B}})\\
&+|R\rangle_{\mathrm{T}}^{\mathrm{P_2}}(\chi|H\rangle_{\mathrm{A}}-\delta|V\rangle_{\mathrm{A}})(\alpha|H\rangle_{\mathrm{B}}-\beta|V\rangle_{\mathrm{B}})\\
&+|L\rangle_{\mathrm{T}}^{\mathrm{P_2}}(\chi|H\rangle_{\mathrm{A}}+\delta|V\rangle_{\mathrm{A}})(\alpha|H\rangle_{\mathrm{B}}+\beta|V\rangle_{\mathrm{B}})\\
&+|R\rangle_{\mathrm{T}}^{\mathrm{Q_2}}(\chi|V\rangle_{\mathrm{A}}-\delta|H\rangle_{\mathrm{A}})(\beta|H\rangle_{\mathrm{B}}-\alpha|V\rangle_{\mathrm{B}})\\
&+|L\rangle_{\mathrm{T}}^{\mathrm{Q_2}}(\chi|V\rangle_{\mathrm{A}}+\delta|H\rangle_{\mathrm{A}})(\beta|H\rangle_{\mathrm{B}}+\alpha|V\rangle_{\mathrm{B}})\Big].
\end{aligned}
\tag{23}
$$

Now, Bob measures the path and the polarization of photon T on the basis of $\{|R\rangle_{\mathrm{T}}\equiv|+\rangle,|L\rangle_{\mathrm{T}}\equiv|-\rangle\}$ using the P-Ds (P-D01∼04). After this measurement is carried out, Alice's photon A and Bob's photon B are simultaneously collapsed to Bob's and Alice's photons B and A, respectively, as shown in Table 1. Through subsequent classical communication, Alice and Bob share information on the initial path, the measured path, and the polarization of photon T. To reconstruct the two simultaneously teleported unknown photons, Alice and Bob perform the appropriate unitary operations U_{A} and U_{B} on photons A and B, respectively, according to the shared information shown in Table 1. Consequently, Alice and Bob achieve the BQTP of two unknown photons using path-polarization intra-particle hybrid entanglement (by transferring a single photon T) and CU gates, which are composed of the consecutive operation of the C-path gate and the G-path gate via XKNLs.

Let us assume that Alice wants to teleport an unknown photon $|\psi\rangle_{\mathrm{A}}=\alpha|H\rangle_{\mathrm{A}}+\beta|V\rangle_{\mathrm{A}}$, and Bob wants to teleport an unknown photon $|\varphi\rangle_{\mathrm{B}}=\chi|H\rangle_{\mathrm{B}}+\delta|V\rangle_{\mathrm{B}}$. Alice transmits photon T along path P $\left(|H\rangle_{\mathrm{T}}^{\mathrm{P}}\right)$. Subsequently, if Bob obtains the measurement outcomes $|L\rangle_{\mathrm{T}}^{\mathrm{P_2}}$ of photon T, then photons A and B are collapsed to $(\chi|V\rangle_{\mathrm{A}}+\delta|H\rangle_{\mathrm{A}})\otimes(\beta|H\rangle_{\mathrm{B}}+\alpha|V\rangle_{\mathrm{B}})$. After the information on the initial path, the measured path, and the measured polarization (P, $\mathrm{P_2}$, and $|L\rangle_{\mathrm{T}}$) of T is shared through classical communication, Alice and Bob perform $U_{\mathrm{A}}=\sigma_X^{\mathrm{A}}$ and $U_{\mathrm{B}}=\sigma_X^{\mathrm{B}}$ on photons A and B, respectively. Consequently, Alice and Bob can simultaneously reconstruct each other's unknown photons $\chi|H\rangle_{\mathrm{A}}+\delta|V\rangle_{\mathrm{A}}$ and $\alpha|H\rangle_{\mathrm{B}}+\beta|V\rangle_{\mathrm{B}}$.

Table 1. The collapsed output photon states of A and B (the simultaneously teleported photons) and the unitary operators U_{A} and U_{B} used to reconstruct the simultaneously teleported photons A and B, depending on Alice's path and Bob's measurement outcomes.

Initial path of Alice	Measured path of Bob	Measured polarization of Bob in photon T	Simultaneously teleported photons A and B	Unitary operators $U_{\mathrm{A}},U_{\mathrm{B}}$ to reconstruct photons A and B
P	$\mathrm{P_1}$	$\|R\rangle_{\mathrm{T}}$	$(\chi\|V\rangle_{\mathrm{A}}+\delta\|H\rangle_{\mathrm{A}})\otimes(\beta\|H\rangle_{\mathrm{B}}+\alpha\|V\rangle_{\mathrm{B}})$	$\sigma_X^{\mathrm{A}}\otimes\sigma_X^{\mathrm{B}}$
		$\|L\rangle_{\mathrm{T}}$	$(\chi\|V\rangle_{\mathrm{A}}-\delta\|H\rangle_{\mathrm{A}})\otimes(\beta\|H\rangle_{\mathrm{B}}-\alpha\|V\rangle_{\mathrm{B}})$	$\mathrm{i}\sigma_Y^{\mathrm{A}}\otimes-\mathrm{i}\sigma_Y^{\mathrm{B}}$
	$\mathrm{Q_1}$	$\|R\rangle_{\mathrm{T}}$	$(\chi\|H\rangle_{\mathrm{A}}+\delta\|V\rangle_{\mathrm{A}})\otimes(\alpha\|H\rangle_{\mathrm{B}}+\beta\|V\rangle_{\mathrm{B}})$	$I^{\mathrm{A}}\otimes I^{\mathrm{B}}$
		$\|L\rangle_{\mathrm{T}}$	$(\chi\|H\rangle_{\mathrm{A}}-\delta\|V\rangle_{\mathrm{A}})\otimes(\alpha\|H\rangle_{\mathrm{B}}-\beta\|V\rangle_{\mathrm{B}})$	$\sigma_Z^{\mathrm{A}}\otimes\sigma_Z^{\mathrm{B}}$
	$\mathrm{P_2}$	$\|R\rangle_{\mathrm{T}}$	$(\chi\|V\rangle_{\mathrm{A}}-\delta\|H\rangle_{\mathrm{A}})\otimes(\beta\|H\rangle_{\mathrm{B}}-\alpha\|V\rangle_{\mathrm{B}})$	$\mathrm{i}\sigma_Y^{\mathrm{A}}\otimes-\mathrm{i}\sigma_Y^{\mathrm{B}}$
		$\|L\rangle_{\mathrm{T}}$	$(\chi\|V\rangle_{\mathrm{A}}+\delta\|H\rangle_{\mathrm{A}})\otimes(\beta\|H\rangle_{\mathrm{B}}+\alpha\|V\rangle_{\mathrm{B}})$	$\sigma_X^{\mathrm{A}}\otimes\sigma_X^{\mathrm{B}}$
	$\mathrm{Q_2}$	$\|R\rangle_{\mathrm{T}}$	$(\chi\|H\rangle_{\mathrm{A}}-\delta\|V\rangle_{\mathrm{A}})\otimes(\alpha\|H\rangle_{\mathrm{B}}-\beta\|V\rangle_{\mathrm{B}})$	$\sigma_Z^{\mathrm{A}}\otimes\sigma_Z^{\mathrm{B}}$
		$\|L\rangle_{\mathrm{T}}$	$(\chi\|H\rangle_{\mathrm{A}}+\delta\|V\rangle_{\mathrm{A}})\otimes(\alpha\|H\rangle_{\mathrm{B}}+\beta\|V\rangle_{\mathrm{B}})$	$I^{\mathrm{A}}\otimes I^{\mathrm{B}}$
Q	$\mathrm{P_1}$	$\|R\rangle_{\mathrm{T}}$	$(\chi\|H\rangle_{\mathrm{A}}+\delta\|V\rangle_{\mathrm{A}})\otimes(\alpha\|H\rangle_{\mathrm{B}}+\beta\|V\rangle_{\mathrm{B}})$	$I^{\mathrm{A}}\otimes I^{\mathrm{B}}$
		$\|L\rangle_{\mathrm{T}}$	$(\chi\|H\rangle_{\mathrm{A}}-\delta\|V\rangle_{\mathrm{A}})\otimes(\alpha\|H\rangle_{\mathrm{B}}-\beta\|V\rangle_{\mathrm{B}})$	$\sigma_Z^{\mathrm{A}}\otimes\sigma_Z^{\mathrm{B}}$
	$\mathrm{Q_1}$	$\|R\rangle_{\mathrm{T}}$	$(\chi\|V\rangle_{\mathrm{A}}+\delta\|H\rangle_{\mathrm{A}})\otimes(\beta\|H\rangle_{\mathrm{B}}+\alpha\|V\rangle_{\mathrm{B}})$	$\sigma_X^{\mathrm{A}}\otimes\sigma_X^{\mathrm{B}}$
		$\|L\rangle_{\mathrm{T}}$	$(\chi\|V\rangle_{\mathrm{A}}-\delta\|H\rangle_{\mathrm{A}})\otimes(\beta\|H\rangle_{\mathrm{B}}-\alpha\|V\rangle_{\mathrm{B}})$	$\mathrm{i}\sigma_Y^{\mathrm{A}}\otimes-\mathrm{i}\sigma_Y^{\mathrm{B}}$
	$\mathrm{P_2}$	$\|R\rangle_{\mathrm{T}}$	$(\chi\|H\rangle_{\mathrm{A}}-\delta\|V\rangle_{\mathrm{A}})\otimes(\alpha\|H\rangle_{\mathrm{B}}-\beta\|V\rangle_{\mathrm{B}})$	$\sigma_Z^{\mathrm{A}}\otimes\sigma_Z^{\mathrm{B}}$
		$\|L\rangle_{\mathrm{T}}$	$(\chi\|H\rangle_{\mathrm{A}}+\delta\|V\rangle_{\mathrm{A}})\otimes(\alpha\|H\rangle_{\mathrm{B}}+\beta\|V\rangle_{\mathrm{B}})$	$I^{\mathrm{A}}\otimes I^{\mathrm{B}}$
	$\mathrm{Q_2}$	$\|R\rangle_{\mathrm{T}}$	$(\chi\|V\rangle_{\mathrm{A}}-\delta\|H\rangle_{\mathrm{A}})\otimes(\beta\|H\rangle_{\mathrm{B}}-\alpha\|V\rangle_{\mathrm{B}})$	$\mathrm{i}\sigma_Y^{\mathrm{A}}\otimes-\mathrm{i}\sigma_Y^{\mathrm{B}}$
		$\|L\rangle_{\mathrm{T}}$	$(\chi\|V\rangle_{\mathrm{A}}+\delta\|H\rangle_{\mathrm{A}})\otimes(\beta\|H\rangle_{\mathrm{B}}+\alpha\|V\rangle_{\mathrm{B}})$	$\sigma_X^{\mathrm{A}}\otimes\sigma_X^{\mathrm{B}}$

For this scheme, we discuss two types of noise in the quantum channel. Such noise occurs when only a single photon T in state $|\Phi\rangle_{\text{Alice}}$ (as given in Eq. (20)) is directly transmitted to Bob, while photon A remains with Alice. For the first type of noise, while Alice stores photon A and transfers photon T to Bob (who stores this photon), the photons in the entangled state (inter-particle entanglement between A and T) may be subject to noise. Oh *et al.*[36] investigated the QTP scheme in noisy channels by analytically and numerically solving a master equation in the Lindblad form Ref. [66]. Subsequently, they examined the average fidelity's characteristic dependence on noise that occurred during QTP. Thereafter, various studies involving QTP protocols investigated noise.[37,39] For the second type of noise, when photon T (a single photon) is transferred from Alice to Bob, this photon is influenced by unavoidable absorption and scattering (noise) in a quantum channel. Amplifying the signal can, in principle, compensate for inevitable transmission losses. One of the most effective ways to overcome the difficulty associated with exponential fidelity decay is photon noiseless linear amplification.[67–72] Consequently, photon amplifiers promise to extend the applicability of quantum information processing protocols[40–42] and to improve the feasibility of our BQTP scheme.

4. Conclusion

We propose an arbitrary CU gate and a BQTP scheme. Our BQTP scheme (in Section 3) uses path-polarization intra-particle hybrid entanglement to simultaneously teleport two unknown photons between users Alice and Bob. For simultaneous teleportation, Alice directly transmits only one photon T to Bob, which is in an intra-particle hybrid entangled state of the path and polarization. Such an entangled state is achieved through a BS and an SF. Subsequently, two unknown photons A and B from Alice and Bob, respectively, are teleported by using linear optical devices and performing CU gates (using XKNLs) on photon T.

In addition to intra-particle hybrid entanglement (which is utilized in our scheme), inter-particle hyperentanglement[73–75] (a different type of hybrid entanglement) is composed of a tensor product with correlations between the two photons' various degrees of freedom. Such degrees of freedom include polarization, momentum, time bin, spatial modes, and energy-time. Inter-particle hyperentanglement can be exploited in a diverse range of quantum information processing protocols, such as photonic quantum computation,[28] deterministic Bell-state measurements,[29,30] entanglement purification and concentration schemes,[31–33] and quantum communications (UQTP schemes)[34,35] via linear optical devices,[29,31] XKNLs,[32–34] and quantum dots in optical micro cavities.[28,30,35]

Compared with existing BQTP schemes[23–27] (in which the inter-particle entanglement of five or more particles is pre-shared among users of a quantum channel), our BQTP scheme constructs the quantum channel during the teleportation procedure by transmitting only one photon T (intra-particle hybrid entanglement). For the quantum channel, our scheme (using intra-particle hybrid entanglement) does not require a preliminary process in which the entangled state is shared between users. From the perspective of a quantum channel, UQTP schemes that use inter-particle hyperentanglement via XKNLs[34] and optical cavities[35] require the pre-sharing of the entangled state (inter-particle hyperentanglement). Furthermore, compared with UQTP schemes using inter-particle hyperentanglement,[34,35] our scheme provides a bidirectional communication process in which Alice and Bob can simultaneously teleport two unknown photons by transmitting only a single photon. Consequently, Alice and Bob simultaneously become both message senders and message receivers. The comparison with these QTP schemes is summarized in Table 2.

Because the BQTP scheme is based on the CU gate, the success probability and feasibility of realization of the proposed scheme (BQTP) strongly depend on the deterministic performance and the experimental implementation of the CU gate. Thus, we propose a nearly deterministic CU gate, which can be operated by the consecutive performance of C-path[57] and G-path gates via weak XKNLs, X-homodyne detections, and feed-forwards, as described in Section 2. The error probability of the single CU gate is $P_{\text{error}}^{\text{CU}} = P_{\text{error}}^{\text{CP}} + P_{\text{error}}^{\text{GP}} - \left(P_{\text{error}}^{\text{CP}} \cdot P_{\text{error}}^{\text{GP}}\right)$, where $P_{\text{error}} = \frac{1}{2}\left[1 - \text{erf}\left(X_{\text{d}}/2\sqrt{2}\right)\right]$ is the error probability induced by the overlap between the two Gaussian curves $f(X,\beta)$ and $f(X,\beta\cos\theta)$. If both the C-path gate and the G-path gate employ the same amplitudes (strong and $\alpha = \alpha'$) of the coherent states and the same phase shift (weak) of the XKNLs, then $P_{\text{error}}^{\text{CP}}$ is equal to $P_{\text{error}}^{\text{GP}}$ in Eq. (16). Thus, the CU gate has $P_{\text{error}}^{\text{CU}} = 2P_{\text{error}}^{\text{GP}} - \left(P_{\text{error}}^{\text{GP}}\right)^2 < 6.8 \times 10^{-6}$ (nearly

Table 2. Comparison with the UQTP and BQTP schemes.

	Unidirectional QTP (UQTP)		Bidirectional QTP (BQTP)	
	Sheng *et al.*[34]	Ren *et al.*[35]	Ref. [23]– [27]	Our scheme
Entanglement	inter-particle hyperentanglement		inter-particle entanglement	intra-particle hybrid entanglement
Quantum gates	XKNLs	Cavities	–	XKNLs
Quantum channel	pre-shared	pre-shared	pre-shared	during procedure
Particles for quantum channel	two photons	two photons	more than five qubits	one photon

deterministic) for $\alpha\theta^2 > 9$. However, natural XKNLs are extremely weak.[76] Hence, it is difficult to discriminate the two overlapping coherent states, which decreases the success probability $P_{\rm succ}^{\rm CU}$ of the CU gate. Fortunately, much progress has been made on the subjects of the Kerr nonlinearity and homodyne detection.[77,78] In 2003, Hofmann *et al.*[77] showed that a phase shift of π can be achieved with a single two-level atom in a one-sided cavity and the displacement-controlled photon-number-resolving (PNR) detector used in Ref. [78]. Consequently, it is possible to achieve deterministic distinguishability between the shifted and non-shifted phases in the coherent state, when the requirement $\alpha\theta^2 \gg 1$ is satisfied. This means that a weak XKNL $\theta \ll 1$ with a sufficiently large amplitude of the probe beam (coherent state) would be applicable. Additionally, the best XKNL created by electromagnetically induced transparency (EIT) techniques is in the range of weak nonlinearities,[55] and the nonlinearity magnitude could be largely improved with the help of EIT, in the region of $\theta \approx 10^{-2}$.[79] Thus, the CU gate can be experimentally implemented with present techniques. In conclusion, our scheme (BQTP) is experimentally applicable with a certain success probability.

Appendix A: CU gates (CZ gate and CNOT gate) on Alice's side

In Section 2, both the control photon and the target photon in the initial state are in a single path of the CU gate, as shown in Eq. (4). However, on Alice's side of the BQTP, the path of the control photon T is divided into two paths, P and Q, when path-polarization intra-particle hybrid entanglement is generated, as shown in Fig. 4(a). In our BQTP scheme, we use a modified CU gate, such as in Fig. 4(b), which contains a split-path of the control photon T. The details are shown in Fig. A1.

For example, let us assume that the control photon is in a state $\frac{1}{\sqrt{2}}\left(|H\rangle_{\rm T}^{\rm P}+|V\rangle_{\rm T}^{\rm Q}\right)$ and the target photon in $|V\rangle_{\rm A}$. The initial state $|\phi\rangle_{\rm int}$ is given by

$$|\phi\rangle_{\rm int}=\frac{1}{\sqrt{2}}\left(|H\rangle_{\rm T}^{\rm P}|V\rangle_{\rm A}^{3}+|V\rangle_{\rm T}^{\rm Q}|V\rangle_{\rm A}^{3}\right), \tag{A1}$$

where the target photon A is in path 3. When passing through the PBS and the C-path gate, the state is changed to $|\phi\rangle_{\rm CP}$

$$\begin{aligned}|\phi\rangle_{\rm int} &\xrightarrow{\text{PBS (Control photon)}} \frac{1}{\sqrt{2}}\left(|H\rangle_{\rm T}^{\rm Q}|V\rangle_{\rm A}^{3}+|V\rangle_{\rm T}^{\rm Q}|V\rangle_{\rm A}^{3}\right)\\ &\xrightarrow{\text{C-path gate}} |\phi\rangle_{\rm CP}=\frac{1}{\sqrt{2}}\left(|H\rangle_{\rm T}^{\rm Q}|V\rangle_{\rm A}^{3}+|V\rangle_{\rm T}^{\rm Q}|V\rangle_{\rm A}^{4}\right).\end{aligned} \tag{A2}$$

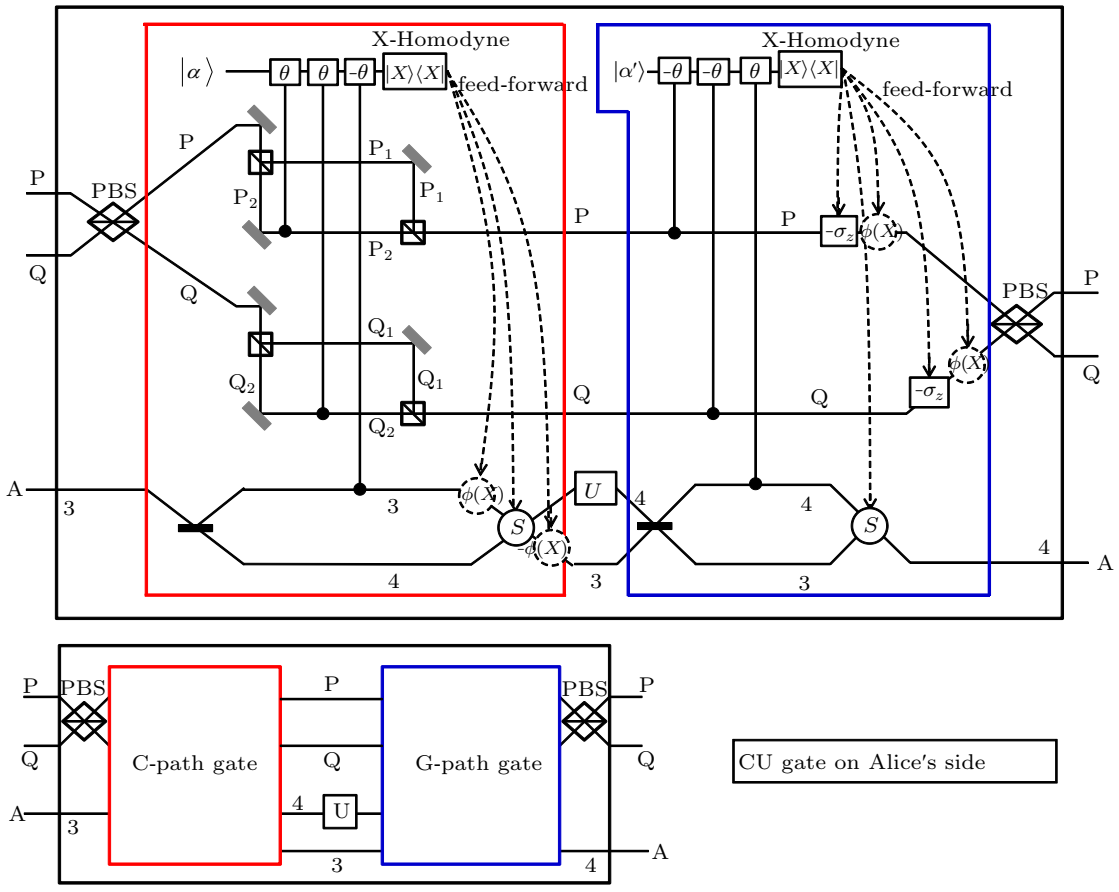


Fig. A1. (color online) The CU gate on Alice's side (Fig. 4(b)): two PBSs, in front of the C-path gate and at the rear of the G-path gate, are utilized to merge and split the path of the control photon T. If the unitary operator U in the middle of the C-path and G-path gates is σ_Z or σ_X, then the CU gate becomes a CZ gate or CNOT gate.

After the application of the unitary operator U, G-path gate, and PBS, the state $|\phi\rangle_{\rm CP}$ is finally transformed to $|\phi\rangle_{\rm fin}$

$$|\phi\rangle_{\rm CP} \xrightarrow{U\ (\text{target photon : path 4})} \frac{1}{\sqrt{2}}\left[|H\rangle_{\rm T}^{\rm Q}|V\rangle_{\rm A}^{3}+|V\rangle_{\rm T}^{\rm Q}\left(U|V\rangle_{\rm A}^{4}\right)\right]$$
$$\xrightarrow{\text{G-path gate}} \frac{1}{\sqrt{2}}\left[|H\rangle_{\rm T}^{\rm Q}|V\rangle_{\rm A}^{4}+|V\rangle_{\rm T}^{\rm Q}\left(U|V\rangle_{\rm A}^{4}\right)\right]$$
$$\xrightarrow{\text{PBS (control photon)}}$$
$$|\phi\rangle_{\rm fin}=\frac{1}{\sqrt{2}}\left[|H\rangle_{\rm T}^{\rm P}|V\rangle_{\rm A}^{4}+|V\rangle_{\rm T}^{\rm Q}\left(U|V\rangle_{\rm A}^{4}\right)\right]. \quad \text{(A3)}$$

If the unitary operator U is σ_Z or σ_X, then the CU gate becomes a CZ gate or CNOT gate

$$U=\sigma_Z \Rightarrow |\phi\rangle_{\rm fin}=\frac{1}{\sqrt{2}}\left(|H\rangle_{\rm T}^{\rm P}|V\rangle_{\rm A}^{4}-|V\rangle_{\rm T}^{\rm Q}|V\rangle_{\rm A}^{4}\right),\ \text{CZ gate},$$

$$U=\sigma_X \Rightarrow |\phi\rangle_{\rm fin}=\frac{1}{\sqrt{2}}\left(|H\rangle_{\rm T}^{\rm P}|V\rangle_{\rm A}^{4}+|V\rangle_{\rm T}^{\rm Q}|H\rangle_{\rm A}^{4}\right),\ \text{CNOT gate}, \quad \text{(A4)}$$

where the initial state is $|\phi\rangle_{\rm int}=\frac{1}{\sqrt{2}}\left(|H\rangle_{\rm T}^{\rm P}|V\rangle_{\rm A}^{3}+|V\rangle_{\rm T}^{\rm Q}|V\rangle_{\rm A}^{3}\right)$ in Eq. (A1).

Appendix B: CU gates (CY gate and CNOT gate) on Bob's side

On Bob's side of the BQTP, the path of the control photon T is divided to four paths, $\rm P_1, P_2, Q_1$, and $\rm Q_2$, as described in Fig. 5(a). In our BQTP scheme, we use a modified CU gate, such as Fig. 5(b), which contains a split-path of the control photon T. The details can be seen in Fig. B1.

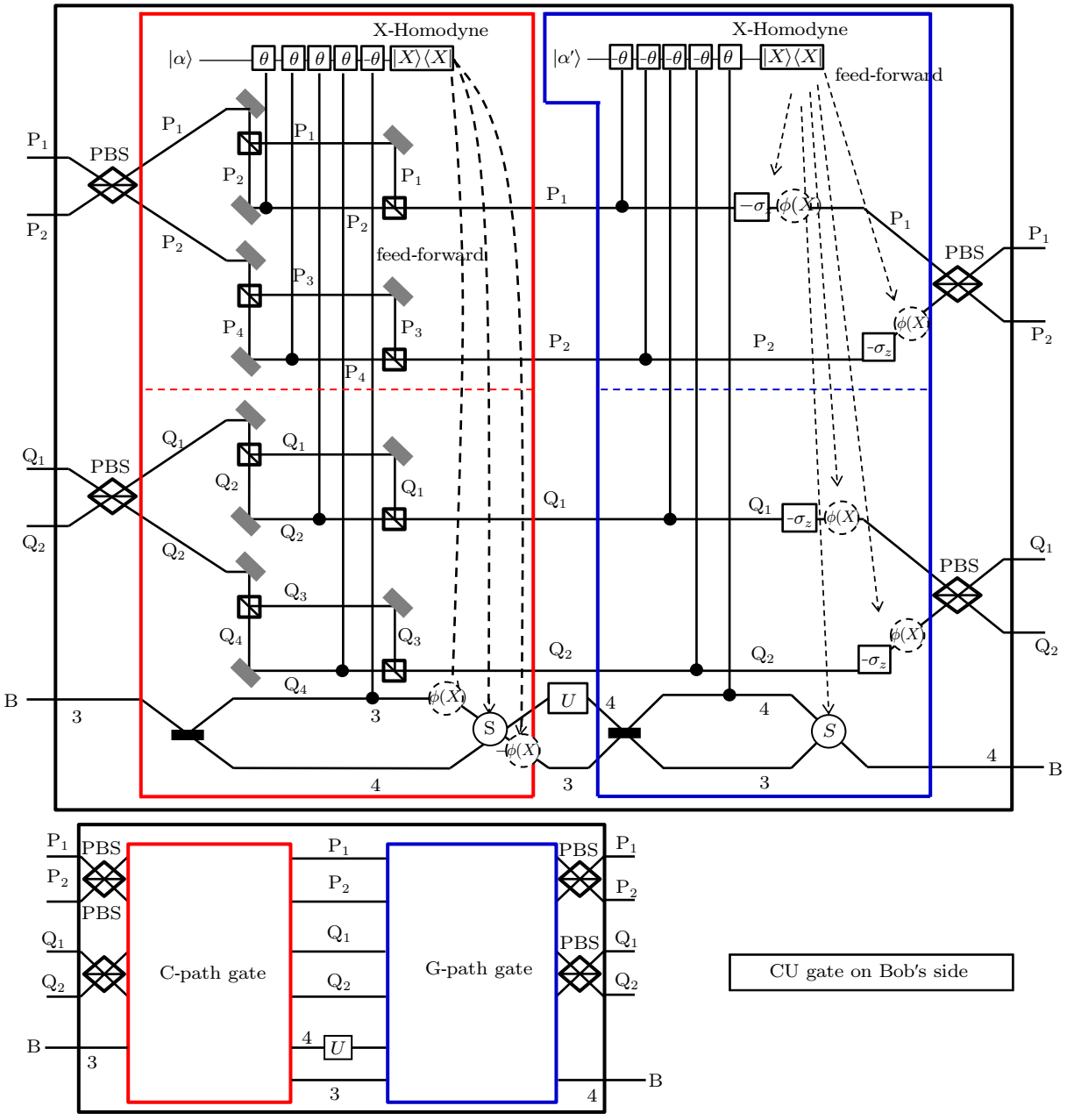


Fig. B1. (color online) The CU gate on Bob's side (Fig. 5(b)): four PBSs in front of the C-path gate and at the rear of the G-path gate are utilized to merge and split the path of the control photon T. If the unitary operator U in the middle of the C-path gate and the G-path gate is $\rm i\sigma_Y$ or σ_X, then the CU gate becomes a CY gate or CNOT gate.

For example, let us assume the control photon state $\frac{1}{2}\left(|H\rangle_{\rm T}^{\rm P_1}+|V\rangle_{\rm T}^{\rm P_2}+|H\rangle_{\rm T}^{\rm Q_1}+|V\rangle_{\rm T}^{\rm Q_2}\right)$ and the target photon state $|H\rangle_{\rm B}$. The initial state $|\vartheta\rangle_{\rm int}$ is given by

$$|\vartheta\rangle_{\rm int}=\frac{1}{2}\Big(|H\rangle_{\rm T}^{\rm P_1}|H\rangle_{\rm B}^{3}+|V\rangle_{\rm T}^{\rm P_2}|H\rangle_{\rm B}^{3}+|H\rangle_{\rm T}^{\rm Q_1}|H\rangle_{\rm B}^{3}+|V\rangle_{\rm T}^{\rm Q_2}|H\rangle_{\rm B}^{3}\Big), \tag{B1}$$

where the path of the target photon B is path 3. Passing through the PBSs and the C-path gate, the state is changed to

$$\begin{aligned}|\vartheta\rangle_{\rm int}&\xrightarrow{\text{PBSs (control photon : path } \rm P_1\text{–}P_2\text{, path } Q_1\text{–}Q_2)}\\&\frac{1}{2}\left(|H\rangle_{\rm T}^{\rm P_2}|H\rangle_{\rm B}^{3}+|V\rangle_{\rm T}^{\rm P_2}|H\rangle_{\rm B}^{3}+|H\rangle_{\rm T}^{\rm Q_2}|H\rangle_{\rm B}^{3}+|V\rangle_{\rm T}^{\rm Q_2}|H\rangle_{\rm B}^{3}\right)\\&\xrightarrow{\text{C-path gate}}|\vartheta\rangle_{\rm CP}=\frac{1}{2}\Big(|H\rangle_{\rm T}^{\rm P_2}|H\rangle_{\rm B}^{3}+|V\rangle_{\rm T}^{\rm P_2}|H\rangle_{\rm B}^{4}\\&\qquad+|H\rangle_{\rm T}^{\rm Q_2}|H\rangle_{\rm B}^{3}+|V\rangle_{\rm T}^{\rm Q_2}|H\rangle_{\rm B}^{4}\Big).\end{aligned} \tag{B2}$$

After the unitary operator U, G-path gate, and the PBSs, the state $|\vartheta\rangle_{\rm CP}$ is finally transformed to

$$\begin{aligned}|\vartheta\rangle_{\rm CP}&\xrightarrow{\text{U (Target photon : path 4)}}\\&\frac{1}{2}\Big[|H\rangle_{\rm T}^{\rm P_2}|H\rangle_{\rm B}^{3}+|V\rangle_{\rm T}^{\rm P_2}\left(U|H\rangle_{\rm B}^{4}\right)+|H\rangle_{\rm T}^{\rm Q_2}|H\rangle_{\rm B}^{3}\\&+|V\rangle_{\rm T}^{\rm Q_2}\left(U|H\rangle_{\rm B}^{4}\right)\Big]\\&\xrightarrow{\text{G-path gate}}\frac{1}{2}\Big[|H\rangle_{\rm T}^{\rm P_2}|H\rangle_{\rm B}^{4}+|V\rangle_{\rm T}^{\rm P_2}\left(U|H\rangle_{\rm B}^{4}\right)\\&\qquad+|H\rangle_{\rm T}^{\rm Q_2}|H\rangle_{\rm B}^{4}+|V\rangle_{\rm T}^{\rm Q_2}\left(U|H\rangle_{\rm B}^{4}\right)\Big]\\&\xrightarrow{\text{PBS (control photon : path } \rm P_1\text{–}P_2\text{, path } Q_1\text{–}Q_2)}\\&|\vartheta\rangle_{\rm fin}=\frac{1}{2}\Big[|H\rangle_{\rm T}^{\rm P_1}|H\rangle_{\rm B}^{4}+|V\rangle_{\rm T}^{\rm P_2}\left(U|H\rangle_{\rm B}^{4}\right)\\&\qquad+|H\rangle_{\rm T}^{\rm Q_1}|H\rangle_{\rm B}^{4}+|V\rangle_{\rm T}^{\rm Q_2}\left(U|H\rangle_{\rm B}^{4}\right)\Big].\end{aligned} \tag{B3}$$

If the unitary operator U is σ_Z or σ_X, then the CU gate becomes a CZ gate or CNOT gate as follows:

$$\begin{aligned}U=\mathrm{i}\sigma_Y\Rightarrow|\vartheta\rangle_{\rm fin}=&\frac{1}{2}\Big(|H\rangle_{\rm T}^{\rm P_1}|H\rangle_{\rm B}^{4}-|V\rangle_{\rm T}^{\rm P_2}|V\rangle_{\rm B}^{4}+|H\rangle_{\rm T}^{\rm Q_1}|H\rangle_{\rm B}^{4}\\&-|V\rangle_{\rm T}^{\rm Q_2}|V\rangle_{\rm B}^{4}\Big),\ \text{CY gate},\\U=\sigma_X\Rightarrow|\vartheta\rangle_{\rm fin}=&\frac{1}{2}\Big(|H\rangle_{\rm T}^{\rm P_1}|H\rangle_{\rm B}^{4}+|V\rangle_{\rm T}^{\rm P_2}|V\rangle_{\rm B}^{4}+|H\rangle_{\rm T}^{\rm Q_1}|H\rangle_{\rm B}^{4}\\&+|V\rangle_{\rm T}^{\rm Q_2}|V\rangle_{\rm B}^{4}\Big),\ \text{CNOT gate},\end{aligned} \tag{B4}$$

where the initial state is

$$|\vartheta\rangle_{\rm int}=\frac{1}{2}\left(|H\rangle_{\rm T}^{\rm P_1}|H\rangle_{\rm B}^{3}+|V\rangle_{\rm T}^{\rm P_2}|H\rangle_{\rm B}^{3}+|H\rangle_{\rm T}^{\rm Q_1}|H\rangle_{\rm B}^{3}+|V\rangle_{\rm T}^{\rm Q_2}|H\rangle_{\rm B}^{3}\right)$$

in Eq. (B1).

References

[1] Ekert A K 1991 *Phys. Rev. Lett.* **67** 661
[2] Bennett C H, Brassard G, Crepeau C, Jozsa R, Peres A and Wootters W K 1993 *Phys. Rev. Lett.* **70** 1895
[3] Hong C H, Heo J, Khym G L, Lim J I, Hong S K and Yang H J 2010 *Opt. Comm.* **284** 2644
[4] Zha X W and Ren K F 2008 *Phys. Rev. A* **77** 014306
[5] Hong C H, Heo J, Lim J I and Yang H J 2010 *Chin. Phys. Lett.* **29** 050303
[6] Bostrom K and Felbinger F 2002 *Phys. Rev. Lett.* **89** 187902
[7] Deng F G and Long G L 2003 *Phys. Rev. A* **68** 042315
[8] Hong C H, Lim J I, Kim J I and Yang H J 2010 *J. Korean Phys. Soc.* **56** 1733
[9] Hong C H, Heo J, Lim J I and Yang H J 2012 *J. Korean Phys. Soc.* **6** 1
[10] Benichi H, Takeda S, Lee N and Furusawa A 2011 *Phys. Rev. A* **84** 012308
[11] Romano R and Loock P 2010 *Phys. Rev. A* **82** 012334
[12] Al-Amri M, Evers J and Suhail Zubairy M 2010 *Phys. Rev. A* **82** 022329
[13] SaiToh A, Rahimi R and Nakahara M 2009 *Phys. Rev. A* **79** 062313
[14] Zha X W and Song H Y 2010 *Commun. Theor. Phys.* **53** 852
[15] Bouwmeester D, Pan J W, Mattle K, Eibl M, Weinfurter H and Zeilinger A 1997 *Nature* **390** 575
[16] Zhao Z, Chen Y A, Zhang A N, Yang T, Briegel H J and Pan JW 2004 *Nature* **430** 54
[17] Riebe M, Hffner H, Roos C F, Hnsel W, Benhelm J, Lancaster G P T, Krber T W, Becher C, Kaler F S, James D F V and Blatt R 2004 *Nature* **429** 734
[18] Karlsson A and Bourennane M 1998 *Phys. Rev. A* **58** 4394
[19] Yang C P, Chu S I and Han S 2004 *Phys. Rev. A* **70** 022329
[20] Deng F G, Li C Y, Li Y S, Zhou H Y and Wang Y 2005 *Phys. Rev. A* **72** 022338
[21] Nie Y Y, Hong Z H, Huang Y B and Yi X J 2009 *Int. J. Theor. Phys.* **48** 1485
[22] Xia Y, Song J, Lu P M and Song H S 2011 *Eur. Phys. J. D* **61** 493
[23] Zha X W, Zou Z C, Qi J X and Song H Y 2012 *Commun. Theor. Phys.* **58** 372
[24] Zha X W, Zou Z C, Qi J X and Song H Y 2013 *Int. J. Theor. Phys.* **52** 1740
[25] Li Y H and Nie L P 2013 *Int. J. Theor. Phys.* **52** 1630
[26] Shukla C, Banerjee A and Pathak A 2013 *Int. J. Theor. Phys.* **52** 3790
[27] Yan A 2013 *Int. J. Theor. Phys.* **52** 3870
[28] Ren B C and Deng F G 2014 *Sci. Rep.* **4** 4623
[29] Wei T C, Barreiro J T and Kwiat P G 2007 *Phys. Rev. A* **75** 060305
[30] Wang T J, Song S Y and Long G L 2012 *Phys. Rev. A* **85** 062311
[31] Ren B C, Du F F and Deng F G 2013 *Phys. Rev. A* **88** 012302
[32] Sheng Y B and Deng F G 2010 *Phys. Rev. A* **81** 032307
[33] Sheng Y B, Zhou L and Zhao S M 2012 *Phys. Rev. A* **85** 044305
[34] Sheng Y B, Deng F G and Long G L 2010 *Phys. Rev. A* **82** 032318
[35] Ren B C, Wei H R, Hua M, Li T and Deng F G 2012 *Opt. Express* **20** 24664
[36] Oh S C, Lee S C and Lee H W 2002 *Phys. Rev. A* **66** 022316
[37] Carlo G, Benenti G and Casati G 2003 *Phys. Rev. Lett.* **91** 257903
[38] Hu M L 2011 *J. Phys. B: At. Mol. Opt. Phys.* **44** 025502
[39] Liang H Q, Liu J M, Feng S S and Chen J G 2013 *Quant Int. Process.* **12** 2671
[40] Chiribella G, Yang Y and Yao A C 2013 *Nat. Commun.* **4** 2915
[41] Lim C C W, Portmann C, Tomamichel M, Renner R and Gisin N 2013 *Phys. Rev. X* **3** 031006
[42] Andersen U L and Ralph T C 2013 *Phys. Rev. Lett.* **111** 050504
[43] Adhikari S, Majumdar A S, Home D and Pan A K 2010 *Europhys. Lett.* **89** 10005
[44] Sun Y, Wen Q Y and Yuan Z 2011 *Opt. Commun.* **284** 527
[45] Pramanik T, Adhikari S, Majumdar A S, Home D and Pan A K 2010 *Phys. Lett. A* **374** 1121
[46] Heo J, Hong C H, Lim J I and Yang H J 2013 *Chin. Phys. Lett.* **30** 040301
[47] Zukowski M and Zeilinger A 1991 *Phys. Lett. A* **155** 69
[48] Ma X S, Qarry A, Kofler J, Jennewein T and Zeilinger A 2009 *Phys. Rev. A* **79** 042101
[49] Boschi D, Branca S, De Martini F, Hardy L and Popescu S 1998 *Phys. Rev. Lett.* **80** 1121
[50] Michler M, Weinfurter H and Zukowski M 2000 *Phys. Rev. Lett.* **84** 5457
[51] Barreiro J T, Wei T C and Kwiat P G 2008 *Nat. Phys.* **4** 282
[52] Hasegawa Y, Loidl R, Badurek G, Baron M and Rauch H 2003 *Nature* **425** 45
[53] Lukin M D and Lu A I 2000 *Phys. Rev. Lett.* **84** 1419

[54] Guo Q, Cheng L Y, Wang H F, Zhang S and Yeon K H 2012 *Opt. Commun.* **285** 1571
[55] Fleischhauer M, Imamoglu A and Marangos J P 2005 *Rev. Mod. Phys.* **77** 633
[56] Nemoto K and Munro W J 2004 *Phys. Rev. Lett.* **93** 250502
[57] Lin Q and Li J 2009 *Phys. Rev. A* **79** 022301
[58] Sheng Y B, Deng F G and Zhou H Y 2008 *Phys. Rev. A* **77** 042308
[59] Zhou J, Yang M, Lu Y and Cao Z L 2009 *Chin. Phys. Lett.* **26** 100301
[60] Guo Q, Bai J, Cheng L Y, Shao X Q, Wang H F and Zhang S 2011 *Phys. Rev. A* **83** 054303
[61] Xiu X M, Dong L, Gao Y J and Yi X X 2012 *Quant. Int. Comput.* **12** 0159
[62] Zheng C H, Zhao J, Shi P, Li W D and Gu Y J 2014 *Opt. Commun.* **316** 26
[63] Zhao R T, Guo Q, Cheng L Y, Sun L L, Wang H F and Zhang S 2013 *Chin. Phys. B* **22** 030313
[64] Barrett S D, Kok P, Nemoto K, Beausoleil R G, Munro W J and Spiller T P 2005 *Phys. Rev. A* **71** 060302
[65] Gardiner C W and Zoller P 2000 *Quantum* Noise (Berlin: Springer Verlag)
[66] Lindblad G 1976 *Math. Phys.* **48** 119
[67] Xiang G Y, Ralph T C, Lund A P, Walk N and Pryde G J 2010 *Nat. Photon.* **4** 316
[68] Ferreyrol F, Barbieri M, Blandino R, Fossier S, Tualle-Brouri R and Grangier P 2010 *Phys. Rev. Lett.* **104** 123603
[69] Zavatta A, Fiurášek J and Bellini M 2010 *Nat. Photon.* **5** 52
[70] Usuga M A, Müller C R, Wittmann C, Marek P, Filip R, Marquardt C, Leuchs G and Andersen U L 2010 *Nat. Phys.* **6** 767
[71] Osorio C I 2012 *Phys. Rev. A* **86** 023815
[72] Kocsis S, Xiang G Y, Ralph T C and Pryde G L 2013 *Nat. Phys.* **9** 23
[73] Barreiro J T, Langford N K, Peters N A and Kwiat P G 2005 *Phys. Rev. Lett.* **95** 260501
[74] Barbieri M, Cinelli C, Mataloni P and De Martini F 2005 *Phys. Rev. A* **72** 052110
[75] Vallone G, Ceccarelli R, De Martini F and Mataloni P 2009 *Phys. Rev. A* **79** 030301
[76] Kok P, Munro W J, Nemoto K, Ralph T C, Dowing J P and Milburn G J 2007 *Rev. Mod. Phys.* **79** 135
[77] Hofmann H F, Kojima K, Takeuchi S and Sasaki K 2003 *J. Opt. B* **5** 218
[78] Wittmann C, Andersen U L, Takeoka M, Sych D and Leuchs G 2010 *Phys. Rev. A* **81** 062338
[79] Lukin M D and Lu A I 2001 *Nature* **413** 273